



### **Science Arts & Métiers (SAM)**

is an open access repository that collects the work of Arts et Métiers Institute of Technology researchers and makes it freely available over the web where possible.

This is an author-deposited version published in: <https://sam.ensam.eu>  
Handle ID: <http://hdl.handle.net/10985/21735>

#### **To cite this version :**


Joseph BASEL, Emeline SIMONETTI, Elena BERGAMINI, Helene PILLET - On the impact of the erroneous identification of inertial sensors' locations on segments and whole-body centers of mass accelerations: a sensitivity study in one transfemoral amputee - Medical & Biological Engineering & Computing - Vol. 59, n°10, p.2115-2126 - 2021

Any correspondence concerning this service should be sent to the repository

Administrator : [scienceouverte@ensam.eu](mailto:scienceouverte@ensam.eu)



# On the impact of the erroneous identification of inertial sensors' locations on segments and whole-body centers of mass accelerations: a sensitivity study in one transfemoral amputee

Joseph Basel<sup>1,2</sup> · Emeline Simonetti<sup>1,2,3</sup>  · Elena Bergamini<sup>2</sup> · H       Pille  <sup>1</sup>

## Abstract

The kinematics of the body center of mass (bCoM) may provide crucial information supporting the rehabilitation process of people with transfemoral amputation. The use of magneto-inertial measurement units (MIMUs) is promising as it may allow in-the-field bCoM motion monitoring. Indeed, bCoM acceleration might be obtained by fusing the estimated accelerations of body segments' centers of mass (sCoM), the formers being computed from the measured accelerations by segment-mounted MIMUs and the known relative position between each pair of MIMU and underlying sCoM. This paper investigates how erroneous identifications of MIMUs positions impact the accuracy of estimated 3D sCoM and bCoM accelerations in transfemoral amputee gait. Using an experimental design approach, 2<sup>15</sup> simulations of erroneous identifications of MIMUs positions (up to 0.02 m in each direction) were simulated over seven recorded gait cycles of one participant. MIMUs located on the trunk and sound lower limbs were shown to explain up to 77% of the variance in the accuracy of the estimated bCoM acceleration, presumably due to the higher mass and/or angular velocity of these segments during gait of lower-limb amputees. Therefore, a special attention should be paid when identifying the positions of MIMUs located on segments contributing the most to the investigated motion.

**Keywords** Center of mass · Gait analysis · Magneto-inertial measurement unit · Sensitivity analysis · Transfemoral amputees

## 1 Introduction

From a mechanical point of view, the motion of the body center of mass (bCoM) is related to the mechanical actions that are applied to the human body. In this respect, the analysis of bCoM kinematics during gait, and more especially of bCoM acceleration, is of particular relevance. Indeed, it provides information regarding the overall movement strategy, as

well as mechanical energy exchanges and power [1–5]. Such information is crucial when investigating altered human gait patterns, such as in people with lower-limb amputation [4, 6]. Indeed, the parameters derived from the bCoM acceleration allow to quantify the severity of the disability or functional changes occurring along the rehabilitation process, and may thus support the clinical decision process [6, 7]. Parameters derived from the bCoM kinematics are usually obtained from force plates, which allow to retrieve the external forces applied on the body, and therefore, the acceleration of the bCoM from the application of Newton's second law [8, 9], or from the combination of an optoelectronic system and an inertial model using the segmental analysis approach [9–11]. This approach consists in modeling each segment of the body as a rigid solid with known inertial properties, which allows tracking the trajectory of the segment's centers of mass (sCoM) from segment-mounted reflective markers, and then, to estimate the bCoM trajectory through a weighted average of the sCoM trajectories. Both force plates and optical motion capture systems impose the gait analysis to be performed in the laboratory and may not be transferrable to the clinical field. In this context, there is a growing interest for in-the-field

---

✉ Joseph Basel  
joseph.basel@ensam.eu

✉ Emeline Simonetti  
emeline.vacherand@invalides.fr

<sup>1</sup> Arts et M  tiers, Institut de Biom  canique Humaine Georges Charpak (IBHGC), 151 boulevard de l'H  pital, 75013 Paris, France

<sup>2</sup> Interuniversity Centre of Bioengineering of the Human Neuromusculoskeletal System (BOHNES), Department of Movement, Human and Health Sciences, University of Rome "Foro Italico", Piazza Lauro de Bosis, 6, 00135 Rome, Italy

<sup>3</sup> Institution Nationale des Invalides (INI)/CERAH, 47 rue de l'Echat, 94000 Cr  teil, France

monitoring of patients' gait, which would allow to quantify walking alterations in a more ecological way with respect to lab-based gait analysis and to assess the needs of patients directly during the rehabilitation, in order to act accordingly, such as by correcting prosthetic alignments [4].

Magneto-inertial measurement units (MIMUs) represent a valuable alternative to lab-based instruments for the quantitative evaluation of gait. MIMUs are wearable, low-cost, small, easy to set up, and self-contained sensors, thus allowing the collection of movement-related information outside the laboratory. They are composed of three axial accelerometers, gyroscopes, and magnetometers which provide, respectively, 3D linear acceleration, angular velocity, and magnetic field vector components. These three signals can be fused to estimate the orientation of the MIMU with respect to an Earth-fixed reference frame [12–15]. Therefore, provided a MIMU is rigidly attached to a body segment, it can be used to estimate the motion of any point of the segment. Indeed, under rigid body assumptions, it is possible to quantify the acceleration of any point of a segment from (i) the known acceleration of a single point pertaining to the segment, (ii) the known angular velocity of the segment, and (iii) the known relative position between both points. In particular, if the position vector of the MIMU with respect to the segment center of mass (sCoM) is known, the sCoM acceleration can be estimated from MIMU data. Thus, if a network of MIMUs located on multiple body segments is used, the bCoM acceleration can be estimated from a weighted sum of the MIMU-based sCoM accelerations following the segmental analysis method [16–18]. In light of the above, it is clear that the accurate determination of the position of each MIMU with respect to the relevant sCoM is crucial to obtain an accurate estimation of 3D sCoM and bCoM acceleration. Obtaining information about the sensitivity of the accuracy of sCoM and bCoM 3D acceleration estimation to erroneous identification of MIMU locations is thus of great interest. While several authors have investigated the suitability of using wearable sensor networks for the estimation of bCoM kinematics using the segmental analysis paradigm [16, 17], including participants with transfemoral amputation [18], none has directly studied the impact of erroneous positioning of MIMUs on segments or on erroneous identification of MIMUs locations. It should be however noted that Tan and coworkers investigated the influence of placement errors of MIMUs on the accuracy of the ground reaction force (GRF) estimated from a machine learning approach in healthy subjects [19]. In their machine learning framework, GRFs were estimated from raw MIMU data, expressed in their respective MIMU local frame, rather than in a common reference frame. Therefore, the estimated GRF components may be affected by errors in both the position and the orientation of MIMUs on body segments. In their study, MIMU locations were moved by  $\pm 0.1$  m along each axis of the body segment and rotated of up to  $25^\circ$  about the same axes in a “one-at-a-time” sensitivity analysis; i.e., the impact on the

estimated GRF of each change of position or orientation of each MIMU was analyzed individually. Position errors were shown to reduce the estimation accuracy of GRF components by up to 6%. The different approach used in their study for the estimation of the GRF components, that is, using a machine learning approach rather than a segmental analysis approach, compromises the transferability of their results to segmental analysis-based approaches. Furthermore, MIMUs data were simulated from reflective markers trajectories in healthy subjects. Little is known about the generalizability of these results when real MIMU data are employed and/or in case of altered walking patterns, such as those of people with lower-limb amputation. Lastly, as the authors used a “one-at-a-time” sensitivity analysis, the effect of errors affecting multiple MIMUs simultaneously was not investigated. Yet, the simultaneous errors made on several MIMUs may affect the accuracy of the estimated bCoM acceleration differently than if only one MIMU were affected by an error (interaction effect). Gaining insight into the effect of simultaneous mislocalizations of multiple segment-mounted MIMUs on the estimated bCoM acceleration is therefore of great interest.

This work aims at contributing filling this gap through the investigation of the impacts of erroneous identification of segment-mounted MIMU positions on the estimated sCoM and bCoM accelerations during walking of a person with transfemoral amputation. To achieve this aim, a mixed experimental/simulation approach was used. First, experimental data were collected using a set of segment-mounted MIMUs to estimate sCoM acceleration during gait using the rigid body assumption and the knowledge of MIMUs/sCoM relative positions in an Earth-fixed reference frame. A weighted average of MIMU-based sCoM accelerations allowed to estimate bCoM acceleration. MIMU-based sCoM and bCoM accelerations were then compared to reference accelerations obtained using optical motion capture and force plate data. Finally, simulated errors in the relative position of MIMUs and their respective sCoM were introduced to quantify the impact of simultaneous erroneous identification of MIMUs positions on the accuracy of sCoM and bCoM acceleration estimates through a sensitivity analysis. The results of the present study are expected to allow the identification of segment-mounted MIMUs for which location errors are the most critical for sCoM and bCoM acceleration estimation. Such results will allow to provide recommendations regarding MIMU positioning and localization over body segments.

## 2 Methods

### 2.1 Experimental method

This study was approved by the local ethical committee (Comité de Protection des Personnes (18/02/2015), CPP

NX06036). A transfemoral amputee subject (mass: 83.1 kg, height: 1.69 m) gave his written informed consent to participate to the study. He was equipped with a set of 5 MIMUs (Xsens Technologies B.V., Enschede, The Netherlands, 100 Hz) located on the trunk (over the sternum), both prosthetic and sound thighs (ThighP, ThighS) and shanks (ShankP, ShankS), as these segments were shown to contribute the most to the bCoM acceleration in people with transfemoral amputation [18, 20]. Each MIMU was inserted in a customized 3D-printed rigid support equipped with 4 reflective markers (Fig. 1). Additionally, as described in Al Abiad et al.'s work [21], 59 reflective markers were positioned on patient's anatomical landmarks, and an optical motion capture system (OMC) was used to record the 3D trajectory of all markers (Vicon system, Oxford Metrics, UK, 100 Hz). The participant was asked to walk in a straight line at his self-selected speed along an 8-m pathway embedding three force plates (AMTI, Advanced Mechanical Technology, Inc., MA, USA, 1000 Hz) located in the middle of the walkway. OMC, force plates, and MIMU data were synchronized with an electronic trigger. Only the prosthetic strides performed at steady state walking speed and occurring on the force plates were considered in the analysis.

## 2.2 Data processing

All raw data from the acquisition were filtered using a Butterworth zero-lag 4th-order low-pass filter with cutoff frequencies set at 5 Hz (MIMUs and markers) and 10 Hz (force plates). Relevant data are available in a data repository [22].

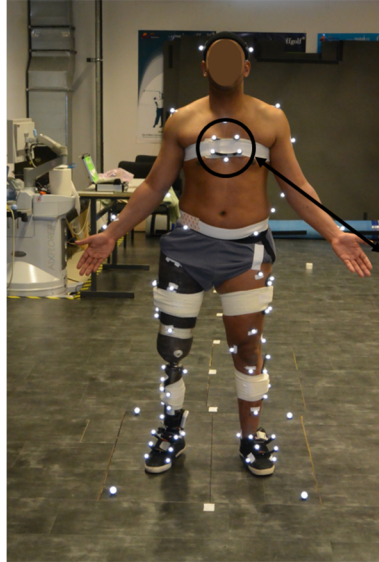


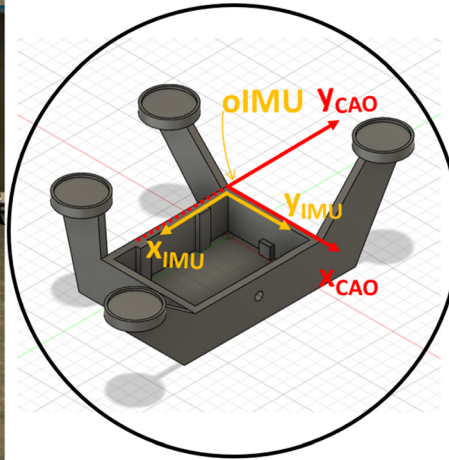
**Fig. 1** Face photo of the subject equipped with the optoelectronic markers and seven MIMUs on the trunk, thighs, shanks, and feet (not used in the present study), with a zoom on the 3D-printed custom rigid support in which was inserted the trunk-mounted MIMU. On the photo, the MIMU/rigid supports were covered with a strap band to avoid sliding of the MIMUs while walking. The 3D-printed rigid support allowed to

### 2.2.1 Reference accelerations

The 3D positions of all sCoM were estimated from OMC measurements combined with a 15-segment inertial model as reported in Pillet et al.'s work [11]. To obtain the reference sCoM accelerations, these positions were differentiated and low-pass filtered using the same Butterworth filter described above with cutoff frequencies set at 8 Hz and 10 Hz for the first and second differentiation, respectively [23]. Reference 3D bCoM acceleration was obtained from the filtered force plate data by dividing the values of the body-weight-subtracted GRF components by the participant's mass. Both sCoM and bCoM reference accelerations were expressed in the OMC inertial reference frame  $R_{OMC}$  such that the  $y$ -axis was aligned with the direction of progression (anteroposterior, AP), the  $z$ -axis vertical and opposing gravity (vertical, V), and the  $x$ -axis orthonormal to both (mediolateral, ML).

### 2.2.2 MIMU-based accelerations

The 3D orientation ( $R_{MIMU}$ ) and position of each MIMU local frame with respect to  $R_{OMC}$  were computed using the markers located on the 3D-printed rigid cluster (Figure 1). Indeed, the 3D-printed rigid cluster was designed such that both the orientation of the MIMU local frame and the orientation of a technical frame defined by the markers positioned on the rigid cluster are known in the computer-aided design reference frame. Therefore, the relative orientation between the MIMU local frame and the technical frame is obtained for each MIMU, which allows in turn to compute the transformation



obtain the position ( $o_{IMU}$ ) and orientation of the MIMU frame ( $x_{IMU}$ ,  $y_{IMU}$ ) relative to the technical frame associated to the 3D-printed support ( $x_{CAO}$ ,  $y_{CAO}$ ). The support was equipped with 4 reflective markers allowing to define the orientation of the MIMU frame in the optical motion capture reference frame during the acquisitions

matrix from  $R_{MIMU}$  to  $R_{OMC}$  obtained and to express both gravity-free accelerations and angular velocities measured by each MIMU in  $R_{OMC}$ .

Then, for each MIMU, the vector connecting the MIMU origin to the center of mass of the underlying segment,  $\overrightarrow{MIMU-sCoM}$ , was obtained in  $R_{OMC}$  using the markers located on the rigid cluster and the sCoM positions derived from the inertial model. MIMU-based estimations of the sCoM accelerations in  $R_{OMC}$ ,  $\overrightarrow{a_{sCoM}^{MIMU}}$ , were then computed as follows:

$$\overrightarrow{a_{sCoM}^{MIMU}} = \overrightarrow{a_{MIMU}} + \frac{d\overrightarrow{\Omega_{MIMU}}}{dt} \wedge \overrightarrow{MIMU-sCoM} + \overrightarrow{\Omega_{MIMU}} \wedge (\overrightarrow{\Omega_{MIMU}} \wedge \overrightarrow{MIMU-sCoM}) \quad (1)$$

with  $\overrightarrow{a_{MIMU}}$  and  $\overrightarrow{\Omega_{MIMU}}$  being the MIMU-measured gravity-free linear acceleration and angular velocity signals expressed in  $R_{OMC}$ .

Finally, bCoM acceleration was estimated as a weighted sum of the estimated sCoM accelerations ( $\overrightarrow{a_{sCoM}^{MIMU}}$ ) following the segmental analysis approach:

$$\overrightarrow{a_{bCoM}^{MIMU}} = \sum_{i=1}^n \frac{m_i}{m_{body}} \overrightarrow{a_{sCoM}^{MIMU}} \quad (2)$$

where  $n$  is the number of segments considered and  $m_{body}$  and  $m_i$  are respectively the masses of the body and of the  $i$ th segment. The accelerations  $\overrightarrow{a_{sCoM}^{MIMU}}$  and  $\overrightarrow{a_{bCoM}^{MIMU}}$  were compared to reference data using the relative root-mean square error ( $rRMSE$ ) [24] and the Pearson's correlation coefficient along AP, ML, and V directions and averaged over the analyzed strides. A significance level of 0.05 was used for the correlations.

### 2.2.3 Sensitivity analysis

A sensitivity analysis was performed to investigate the impact of an erroneous identification of each MIMU location, namely an error on the components of the vector  $\overrightarrow{MIMU-sCoM}$ , on the  $rRMSE$  between MIMU-based and reference sCoM and bCoM accelerations.

To this aim, errors in the identification of MIMU positions on the relevant body segments reaching up to 0.02 m in all three directions (AP, ML, and V) were introduced. This range of errors was estimated experimentally (see the “[Supplementary information](#)” for details). Simulations were performed where each MIMU position was varied from its actual position ( $p_{0AP}$ ,  $p_{0ML}$ ,  $p_{0V}$ ) by  $\pm 0.02$  m along each axis of the  $R_{OMC}$  reference frame. The resulting sCoM accelerations were estimated using the following Equation (3):

$$\overrightarrow{a_{sCoM}^{MIMU}} = \overrightarrow{a_{MIMU}} + \frac{d\overrightarrow{\Omega_{MIMU}}}{dt} \wedge \overrightarrow{MIMU-sCoM} + \overrightarrow{\Delta} + \overrightarrow{\Omega_{MIMU}} \wedge (\overrightarrow{\Omega_{MIMU}} \wedge \overrightarrow{MIMU-sCoM} + \overrightarrow{\Delta}) \quad (3)$$

where  $\overrightarrow{a_{MIMU}}$  and  $\overrightarrow{\Omega_{MIMU}}$  are the linear acceleration and angular velocity measured by the MIMU and expressed in  $R_{OMC}$ , and an erroneous term  $\overrightarrow{\Delta} = (\Delta_{AP}, \Delta_{ML}, \Delta_V)$  was added to the vector  $\overrightarrow{MIMU-sCoM}$  with  $\Delta_i \in \{-0.02 \text{ m}, 0 \text{ m}, 0.02 \text{ m}\}$  for  $i = AP, ML, V$ .

The  $rRMSE$  between the reference- and simulated MIMU-based sCoM and bCoM accelerations, referred hereafter as  $\gamma^{sCoM_i}$  and  $\gamma^{bCoM}$ , was then computed. This allowed to construct a so-called mechanical model for each sCoM or bCoM acceleration component linking the  $rRMSE$  (outputs) to the input errors  $\Delta_i$ .

Using the experimental design methodology [25], the relation between each component of the  $rRMSE$  (AP, ML, V) and the simulated mislocalization of MIMUs along the AP, ML, and V axis (hereafter designated as “factors”) can also be modelled with a polynomial model of degree up to 2 as described in Eq. (4), resulting in three models per MIMU (for the AP, ML, V components of the relevant sCoM acceleration) and for the bCoM:

$$\hat{\gamma}_{stat}^{acc}(X) = b_0 + \sum_{i=1}^n b_i x_i + \sum_{i=1}^n \sum_{j>1} b_{ij} x_i x_j + \sum_{i=1}^n b_{ii} x_i^2 \quad (4)$$

where:  $\hat{\gamma}_{stat}^{acc}$  is the estimated  $rRMSE$  between reference- and MIMU-based accelerations ( $acc$ ) and  $X$  is a vector containing the  $n = 3N$  factors  $x_i$  corresponding to the variations of positions of the  $N$  MIMUs used for the estimation along the three directions ( $N = 1$  for sCoM acceleration and  $N = 5$  for bCoM acceleration). The sensitivity of the  $rRMSE$  to any of the factor  $x_i$  can then be computed based on an analysis of the variance. In order to have meaningful sensitivity indices and interpretable results, the polynomial model must first be validated. To that end, the residual error between the experimental-based simulated data (mechanical model) and the polynomial-based simulated data must first be investigated at a few points, the number of which depends on the degree of the polynomial model.

**Sensitivity of sCoM acceleration estimates** For each MIMU, three polynomial models were devised to emulate the sCoM acceleration along each axis of the OMC inertial reference frame, following eq. (4) with three input factors  $x_i$ :  $p_{AP}$ ,  $p_{ML}$ ,  $p_V$ , corresponding to the simulated localization of each MIMU along the three axes of  $R_{OMC}$ . For  $i = AP, ML, V$ ,  $p_i = p_{0i} + \Delta_i$ , with  $p_{0i}$  the true localization of the  $i$ th MIMU and  $\Delta_i$  the simulated error made in the localization of the MIMU. Then, after normalization of the factors' values into  $[-1; 1]$ , a three-level full factorial design allowed to choose the experimental points resulting in  $3^3$  combinations of the factors (i.e., 27



different position simulations since each of the three factors has three levels, corresponding to the possible values taken by the error term  $\Delta_i$  per MIMU (Table 1).

**Choice of the polynomial model complexity** The model complexity depends on the inclusion of the interaction ( $\sum_{i=1}^n \sum_{j>1} b_{ij} x_i x_j$ ) and/or quadratic terms ( $\sum_{i=1}^n b_{ii} x_i^2$ ) in Equation (4) and therefore on the degree of the polynomial model used to represent the relationship between the  $rRMSE$  and the introduced localization errors. The choice of the model complexity is determined based upon the residual variance between the polynomial model ( $\hat{Y}_{stat}^{sCoM_i}(X)$ ) and the mechanical model ( $Y^{sCoM_i}(X)$ ) and will be justified in Section 3.b.i.

**Quantification of the sensitivities** Based on the experimental design methodology, the influence of each factor (i.e., the coordinate of the simulated MIMU origin along each axis of  $R_{OMC}$ ) on the accuracy of the sCoM acceleration estimate is defined as the total percentage of variance of the output of the polynomial model due to this factor [25]. First, the sensitivity of the output  $\hat{Y}_{stat}^{acc}$  to each monomial (i.e., linear ( $b_i x_i$ ), interaction ( $b_{ij} x_i x_j$ ), or quadratic term ( $b_{ii} x_i^2$ )) of the polynomial model is computed. With the input factors considered independent and uniformly distributed in  $[-1, 1]$ , the following equations can be written:

$$\begin{cases} s_i = \text{var}(b_i x_i) = b_i^2 \text{var}(x_i) = b_i^2 \times \frac{1}{3} \\ s_{ii} = \text{var}\left(b_{ii} x_i^2\right) = b_{ii}^2 \text{var}\left(x_i^2\right) = b_{ii}^2 \times \frac{4}{45} \\ s_{ij} = \text{var}\left(b_{ij} x_i x_j\right) = b_{ij}^2 \text{var}(x_i) \text{var}(x_j) = b_{ij}^2 \times \frac{1}{9} \\ \text{var}\left(\hat{Y}_{stat}^{acc}\right) = \sum_{i=1}^6 s_i + \sum_{i=1}^6 s_{ii} + \sum_{i=1}^6 \sum_{j>i} s_{ij} \end{cases}$$

The sensitivity to the  $i$ th factor  $x_i$  can be obtained as follows:

- $S_i = s_i + \sum_j s_{ij}$  for the linear model with interactions
- $S_i = s_i + \sum_j s_{ij} + s_{ii}$  for the quadratic model with interactions

The sensitivities  $S_i$  were then expressed as a percentage of the total variance ( $\text{var}\left(\hat{Y}_{stat}^{acc}\right)$ ).

**Table 1** Levels of the factors used for each polynomial model emulating a component of a sCoM acceleration

| Factors      | Level of the factors |               |                  |
|--------------|----------------------|---------------|------------------|
|              | Low-level (−1)       | Mid-level (0) | High-level (+1)  |
| $p_{AP}$ (m) | $p_{0AP} - 0.02$     | $p_{0AP}$     | $p_{0AP} + 0.02$ |
| $p_{ML}$ (m) | $p_{0ML} - 0.02$     | $p_{0ML}$     | $p_{0ML} + 0.02$ |
| $p_V$ (m)    | $p_{0V} - 0.02$      | $p_{0V}$      | $p_{0V} + 0.02$  |

**Sensitivity of bCoM acceleration estimations** Three polynomial models of the highest complexity defined for the sCoM models were built for the bCoM acceleration sensitivity analysis following Equation (4) with  $n = 15$  factors corresponding to the three position error factors of each of the five MIMUs. In order to limit the number of simulations ( $k^{15}$  with  $k$  the number of levels per factor), a two-level factorial design (factors taking the levels  $\pm 1$ ) was considered sufficient if the model was linear with interactions, whereas a three-level factorial design (factors taking the levels  $\pm 1$  and 0) was implemented if the model was quadratic with interaction [25]. As for sCoM acceleration models, the suitability of the complexity chosen will be verified using an analysis of the residual variance of the polynomial models compared to that of the mechanical models.

## 3 Results

The experimental protocol allowed to acquire the data from seven complete prosthetic strides recorded by the OMCS, the MIMUs, and the force plates simultaneously. Therefore, seven strides were analyzed in this study.

### 3.1 Reference- and MIMU-based estimations of the bCoM acceleration

Components in AP, ML, and V directions are reported in Fig. 2. The accuracy of the MIMU-based bCoM and sCoM accelerations in terms of  $rRMSE$  values and correlation coefficients compared to the reference accelerations is presented in Table 2. It should be stressed that the MIMU-based estimations presented in Fig. 2 and Table 2 were obtained with the correct identification of the sensor position, i.e., with  $p_{0AP}$ ,  $p_{0ML}$ , and  $p_{0V}$ , as defined with the rigid marker clusters (Fig. 1). Results show relatively low errors ( $< 15.4 \pm 2.5\%$  in AP,  $< 11.8 \pm 1.3\%$  in ML,  $< 12.5 \pm 2.0\%$  in V) and mostly good correlations between reference- and MIMU-based accelerations ( $r > 0.77$ ).

### 3.2 Sensitivity analysis

#### 3.2.1 Sensitivity of sCoM acceleration estimations

**Choice of the polynomial model complexity** Residual variances achieved by the polynomial models developed for the each component of the sCoM acceleration of each segment are presented in Table 3. Both the quadratic and multilinear models with interactions presented low residual variances for all segments and axes ( $\sigma^2 \leq 0.158$ , except for the prosthetic shank in the vertical direction -  $\sigma^2 \leq 0.663$ ) with the lowest values for the quadratic models (Table 3).

Based on these results, the linear model with interactions was considered an optimal compromise between accuracy and simplicity. Indeed, the achieved maximal residual variance with the multilinear models (0.663) represents a standard deviation of  $\sigma = 0.8\%$  which, compared to  $rRMSE$  of the order of 6% (Table 2), was considered largely acceptable. The model complexity corresponding to a first-order polynomial model with interactions was selected for all MIMUs and all acceleration components. Therefore, all results presented hereafter were obtained using models with this complexity.

**Quantification of the sensitivities** The results of the sensitivity analysis for each sCoM acceleration component (AP, ML, V) are summed up in Fig. 3.

For the lower limbs,  $p_{AP}$  was found to be the major influencer for the ML and V components of sCoM acceleration, whereas  $p_V$  was the one for the AP component. Regarding the prosthetic shank, however, the influence of  $p_V$  dominated that of  $p_{AP}$  in

all three directions. The trunk segment displayed a different behavior with respect to the other segments and was the only one where the MIMU mediolateral position  $p_{ML}$  displayed a prominent role. Finally, the interactions between factors showed minor influences on the accelerations' estimation. The most important influence of interaction factors was obtained for the prosthetic shank where the interactions between  $p_{ML}$  and  $p_{AP}$  and between  $p_V$  and  $p_{AP}$  explained 15.1% of the total variance (Fig. 3).

The range of variation of the estimation accuracy  $\Delta_{rRMSE_i}$  (%) caused by simulated errors in the identification of the MIMU positions over all the simulations is presented in Table 4 for each component of sCoM acceleration (AP, ML, V). Errors in the identification of the MIMU positions resulted in changes of the estimation accuracy of SCoM acceleration between  $-1.6\% < \Delta_{rRMSE_{AP}} < +1.7\%$  in AP,  $-1.5\% < \Delta_{rRMSE_{ML}} < +1.6\%$  in ML, and  $-5.6\% < \Delta_{rRMSE_V} < +6.9\%$  in V compared to the  $rRMSE$  obtained when these MIMU positions were correctly identified (Table 2).

**Fig. 2** Comparison of bCoM accelerations obtained with MIMU (straight lines) and force plates (dotted lines) averaged over the trials

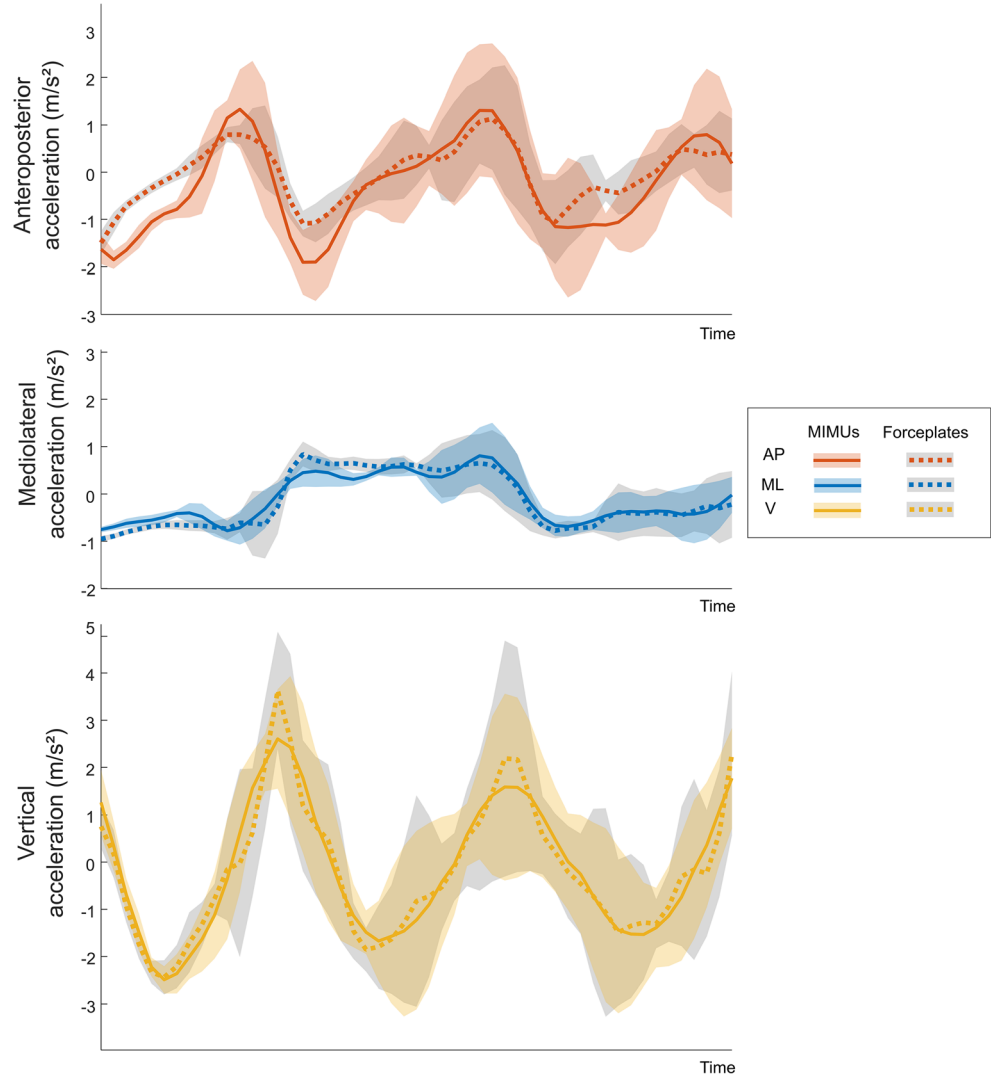


**Table. 2** Comparison of the computed SCoM and BCoM accelerations to reference values, quantified using the average and standard deviation of the NRMSE (%) and Pearson's  $r$  correlations over the 7 trials

|      |            |               | AP          | ML          | V           |
|------|------------|---------------|-------------|-------------|-------------|
| SCoM | Trunk      | NRMSE (%)     | 14.1 (1.9)  | 9.8 (1.2)   | 5.2 (2.3)   |
|      |            | Pearson's $r$ | 0.77 (0.03) | 0.94 (0.02) | 0.98 (0.03) |
|      | ThighS     | NRMSE (%)     | 9.9 (2.2)   | 10.2 (1.3)  | 7.5 (2.0)   |
|      |            | Pearson's $r$ | 0.85 (0.10) | 0.83 (0.08) | 0.93 (0.06) |
|      | ThighP     | NRMSE (%)     | 12.5 (1.5)  | 5.7 (1.9)   | 5.5 (1.2)   |
|      |            | Pearson's $r$ | 0.89 (0.03) | 0.96 (0.03) | 0.97 (0.01) |
|      | ShankS     | NRMSE (%)     | 8 (1.8)     | 10.1 (1.5)  | 12.0 (1.5)  |
|      |            | Pearson's $r$ | 0.94 (0.04) | 0.81 (0.13) | 0.84 (0.05) |
|      | ShankP     | NRMSE (%)     | 4.8 (1.2)   | 5.8 (0.7)   | 12.5 (2.0)  |
|      |            | Pearson's $r$ | 0.98 (0.01) | 0.97 (0.01) | 0.87 (0.04) |
| BCoM | Whole-body | NRMSE (%)     | 15.4 (2.5)  | 11.8 (1.3)  | 8.7 (0.5)   |
|      |            | Pearson's $r$ | 0.93 (0.01) | 0.94 (0.02) | 0.95 (0.01) |

### 3.2.2 Sensitivity of bCoM acceleration estimations

**Choice of the polynomial model complexity** The three multilinear models including interactions developed for the sensitivity analysis of each of the bCoM acceleration component presented low residual variance values, comparable to that of the quadratic model ( $\sigma^2 \leq 10^{-3}$ ) (Table 5).

Consequently, a two-level factorial design was considered to be sufficient to emulate the mechanical models corresponding to the bCoM acceleration. The sensitivity analysis was subsequently performed with the 15 factors of the models resulting in  $2^{15}$  simulations.

**Quantification of the sensitivities** Fig. 4 highlights the factors that have the most influence on the accuracy of the estimation of each component (AP, ML, V) of the bCoM acceleration. For better readability and clarity, only the factors accounting for more than 1% of the total variance are shown in the figure. The bCoM acceleration appears to be mostly sensitive to trunk, sound shank, and sound thigh factors, particularly to the localization errors along AP and V directions. Indeed, all together,  $p_{AP_{Trunk}}$ ,  $p_{V_{Trunk}}$ ,  $p_{AP_{ThighS}}$ ,  $p_{V_{ThighS}}$ ,  $p_{AP_{ShankS}}$  and  $p_{V_{ShankS}}$  explain 92%, 77%, and 79% of the sensitivity of the estimation of the AP, ML, and V bCoM acceleration components, respectively. It should be noted that the anteroposterior localization of the trunk MIMU only has a significant impact

on the ML component of the bCoM acceleration (accounting for 10.5% of the total variance).

Similarly to the sCoM analysis, the  $rRMSE$  ranges of the variation  $\Delta_{rRMSE_i}$  (%) obtained when simulating an error in the identification of MIMUs positions were computed and results are reported in Table 6. The different combinations of errors in the identification of the MIMU positions resulted in changes of the estimation accuracy of the bCoM acceleration between  $-3.4\%$  and  $+2.8\%$  compared to the  $rRMSE$  obtained when these MIMUs positions were correctly identified (Table 6).

## 4 Discussion

The present work investigated the impact of the erroneous identification of the position of five segment-mounted MIMUs on the estimation of the corresponding sCoM and bCoM accelerations.

### 4.1 Reference- and MIMU-based accelerations

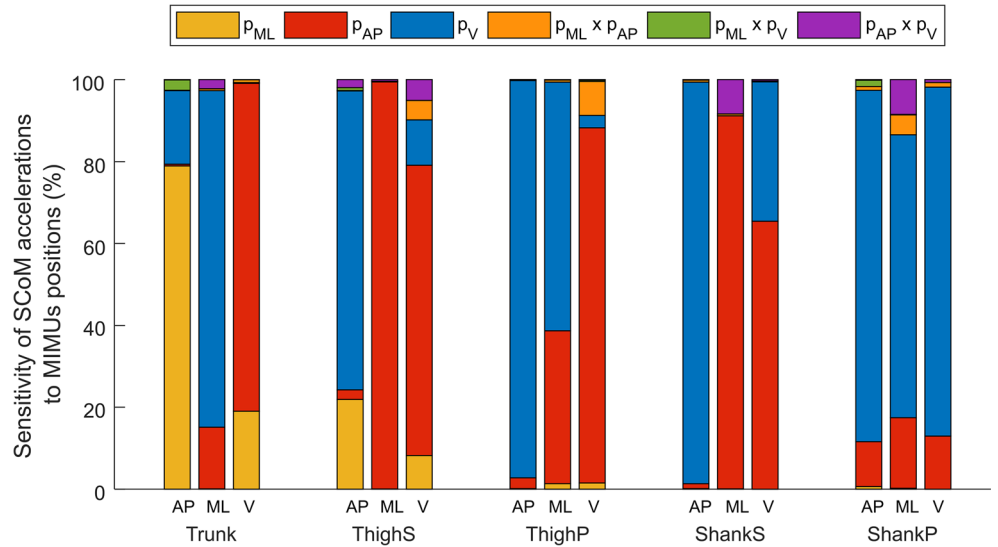
The implemented MIMU-based framework for the estimations of sCoM and bCoM accelerations provided relatively accurate results (high agreement:  $r > 0.77$ , and relatively low errors:  $< 15.4\%$  in AP,  $< 11.8\%$  in ML,  $< 12.5\%$  in V)

**Table. 3** Residual variances  $\sigma^2$  of the linear model with interactions and quadratic model for each segment in the anteroposterior (AP), mediolateral (ML) and vertical (V) directions

| Model                 | $\sigma^2$ (Trunk) |             |             | $\sigma^2$ (ThighS) |       |             | $\sigma^2$ (ThighP) |       |             | $\sigma^2$ (ShankS) |       |       | $\sigma^2$ (ShankP) |             |       |
|-----------------------|--------------------|-------------|-------------|---------------------|-------|-------------|---------------------|-------|-------------|---------------------|-------|-------|---------------------|-------------|-------|
|                       | AP                 | ML          | V           | AP                  | ML    | V           | AP                  | ML    | V           | AP                  | ML    | V     | AP                  | ML          | V     |
| Linear + interactions | $< 10^{-3}$        | 0.095       | 0.004       | 0.010               | 0.147 | 0.152       | 0.046               | 0.044 | 0.158       | 0.032               | 0.143 | 0.134 | 0.082               | 0.065       | 0.663 |
| Quadratic             | $< 10^{-3}$        | $< 10^{-3}$ | $< 10^{-3}$ | $< 10^{-3}$         | 0.001 | $< 10^{-3}$ | $< 10^{-3}$         | 0.001 | $< 10^{-3}$ | $< 10^{-3}$         | 0.002 | 0.002 | $< 10^{-3}$         | $< 10^{-3}$ | 0.097 |



**Fig. 3** Sensitivities of the sCoM accelerations to each factor  $= x_i$  and interactions between factors ( $x_i \times x_j$ ) with  $x_i = \{p_{AP}, p_{ML}, p_V\}$  expressed in percent of the total variance. For each MIMU location, the sensitivities of each component of the sCoM acceleration (AP, ML, V) to the factors are displayed



compared to reference-based acceleration, and showed improved results compared to those obtained in Shahabpoor et al.'s work [16] in healthy participants with a similar methodology. Of course, these values should be considered at the light of the accuracy requirements (and variations) of the specific case under analysis. Overall, sCoM acceleration estimations showed higher agreements at the prosthetic limbs than at the sound limbs. This can be due, in part, to the fact that MIMUs positioned on the prosthetic limb are not affected by soft-tissue artifacts contrary to those positioned on the sound limbs, for which the rigid body assumption is surely weaker.

## 4.2 Sensitivity analysis

Using an experimental design methodology, the sensitivity of each component of the sCoM and bCoM accelerations to

errors in the identification of each MIMU position was estimated using optimal polynomial models.

### 4.2.1 Sensitivity of sCoM acceleration estimations

**Quantification of the sensitivities** The sensitivity analysis allowed to identify the factors having the greatest influence on the accuracy of the acceleration estimates of each sCoM. For the lower limbs, erroneous localization of MIMUs along the AP axis mainly influences the vertical component of the acceleration, whereas incorrect localization along the V axis impacts mainly the ML and AP acceleration components. It is worth noting that, for the prosthetic shank, the vertical localization of the MIMU displays a dominant role over the AP one even for the V component of the acceleration. The localization of MIMUs along the ML direction was shown not to have a

**Table. 4** Range of variation of the SCoM estimation accuracy  $\Delta_{rRMSE_i}$  (%) caused by errors in the identification of the corresponding MIMU positions over all the simulations. Results are presented for each component of SCoM acceleration (AP, ML, V)

| Trunk                                 | AP    | ML    | V     |
|---------------------------------------|-------|-------|-------|
| Lower range of $\Delta_{rRMSE_i}$ (%) | - 0.2 | - 0.7 | - 0.4 |
| Upper range of $\Delta_{rRMSE_i}$ (%) | + 0.2 | + 1.1 | + 0.6 |
| Sound Thigh                           | AP    | ML    | V     |
| Lower range of $\Delta_{rRMSE_i}$ (%) | - 0.5 | - 0.6 | - 1.1 |
| Upper range of $\Delta_{rRMSE_i}$ (%) | + 0.3 | + 0.7 | + 1.1 |
| Prosthetic Thigh                      | AP    | ML    | V     |
| Lower range of $\Delta_{rRMSE_i}$ (%) | - 1.6 | - 1.4 | - 1.1 |
| Upper range of $\Delta_{rRMSE_i}$ (%) | + 1.4 | + 1.5 | + 1.2 |
| Sound Shank                           | AP    | ML    | V     |
| Lower range of $\Delta_{rRMSE_i}$ (%) | - 1.6 | - 1.5 | - 4.2 |
| Upper range of $\Delta_{rRMSE_i}$ (%) | + 1.7 | + 1.6 | + 3.7 |
| Prosthetic Shank                      | AP    | ML    | V     |
| Lower range of $\Delta_{rRMSE_i}$ (%) | - 1.1 | - 0.5 | - 5.6 |
| Upper range of $\Delta_{rRMSE_i}$ (%) | + 1.1 | + 0.8 | + 6.9 |

**Table. 5** Residual variances  $\sigma^2$  of the linear model with interactions and of the quadratic model for each BCoM component

| Model                 | $\sigma^2$ (AP) | $\sigma^2$ (ML) | $\sigma^2$ (V) |
|-----------------------|-----------------|-----------------|----------------|
| Linear + interactions | < 0 .001        | 0.001           | < 0 .001       |
| Quadratic             | < 0 .001        | 0.001           | < 0 .001       |

major impact on the estimation of their corresponding sCoM acceleration, except for the trunk, and to a lesser extent, for the sound thigh. This may be explained by the fact that, during gait, the angular velocity of the lower limbs is mainly directed around the ML axis and has a very low magnitude around the V axis. Consequently, modifications of the lower-limb MIMU positions along the ML axis are not expected to have a major impact on sCoM accelerations (see Equation (1) and the properties of the cross-product). This observation shows that the influence of position identification errors depends on the considered movement/segment. This has to be taken into consideration particularly in altered gait patterns such as those of people with amputation or if movements other than walking in a straight line were studied.

Importantly, erroneous identification of MIMU positions of  $\pm 0.02$  m triggered errors between  $-5.6\% < \Delta_{rRMSE} < +6.9\%$  for all sCoMs and all acceleration components considered, but only between  $-1.6\% < \Delta_{rRMSE} < +1.7\%$  when the shanks are not considered. Considering  $rRMSE$  of the order of 10% between MIMU-based measurement and reference values, these variations cannot be considered negligible, especially for the shanks. The higher impact of erroneous position identification of shank-mounted MIMUs could be explained by the high angular velocity of the shanks compared to the other segments considered. Taken together, these observations suggest that specific attention must be given to the correct identification of the sensor positions, especially for the AP and V directions and for the shank-mounted MIMUs, in order to limit the resulting errors.

#### 4.2.2 Sensitivity of bCoM acceleration estimations

**Quantification of the sensitivities** The results observed for the sensitivity of sCoM acceleration estimations clearly impacted those related to the bCoM acceleration. For a given segment, the component that was shown to be the most influent for the sCoM acceleration estimation accuracy also played a role in that of the bCoM. For instance, erroneous identification of the positions of the sound shank-mounted MIMU along the V direction was found to greatly influence the bCoM acceleration estimates in the AP direction as was observed for the sCoM (Figs. 3 and 4).

Variations in  $rRMSE$  of up to 2.8%, 2.3%, and 1.4% were observed in AP, ML, and V directions respectively. The

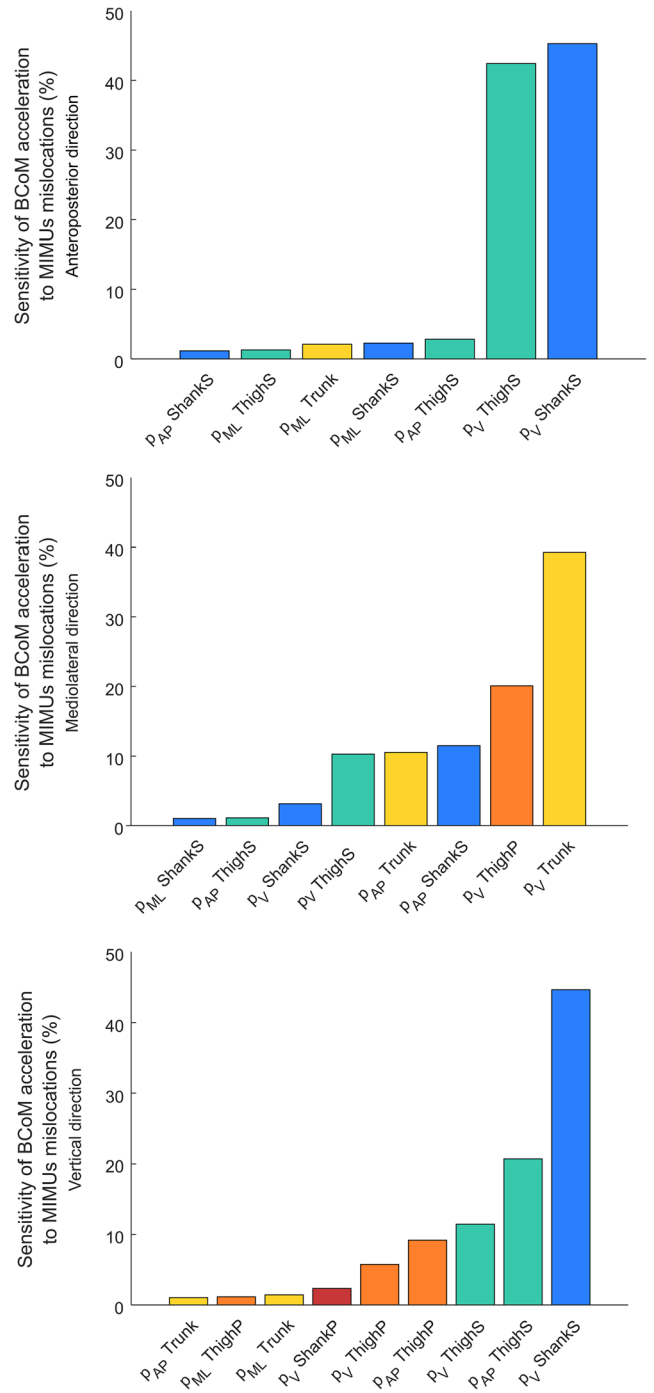


**Fig. 4** Barplot of the results of the sensitivity analysis expressed in percent of total variance for each component of the bCoM acceleration (AP, ML, V). Sensitivities are presented here for the factors  $x_i$  and interactions between factors ( $x_i \times x_j$ ) that account for more than 1% of the total variance

higher  $rRMSE$  variation for the AP and ML components might be explained by the lower amplitude of bCoM acceleration along these directions compared to that along the V direction (Fig. 2). The amplitude of these variations should be interpreted at the light of the accuracy obtained between MIMU- and reference-based acceleration estimation, which

**Table 6** Maximum range of variation of the estimation accuracy  $\Delta_{rRMSE_i}$  (%) caused by errors in the identification of the MIMU positions over all the simulations. Results are presented for each component of BCoM acceleration (AP, ML, V)

|  | AP    | ML    | V    |
|--|-------|-------|------|
| Lower limit for $\Delta_{rRMSE_i}$ (%) | -3.4  | -2.2  | -1.0 |
| Upper limit for $\Delta_{rRMSE_i}$ (%) | + 2.8 | + 2.3 | +1.4 |

were of the order of 15% in ML and AP, and 5% in V (Table 2). It is interesting to note that variations in  $rRMSE$  for the bCoM increased with respect to those of the sCoM only for the AP and ML directions, but not for the V one. This may be due to the fact that for the sCoM accelerations, the maximal variations of  $rRMSE$  along the vertical direction were obtained for the shank segments, which have a lower mass compared to that of the thighs and trunk, especially for the prosthetic side. Therefore, when computing the bCoM acceleration from a weighted sum of the sCoM acceleration, the variability in the shanks sCoM acceleration accuracy has a reduced impact on that of the bCoM.

Comparison of the present results with the existing literature must be performed with caution due to the different methodologies and target parameters. Specifically, Tan and co-workers [19] used a one-at-a-time sensitivity analysis to assess the impact of MIMU placement errors on the estimation of ground reaction force (GRF). In this case, interactions of several MIMU placement errors were not considered. The authors reported that, when a single sensor was misplaced, the accuracy of GRF estimation decreased by up to 0.9%, 2.2%, and 1.1% in the AP, ML, and V directions, respectively. It is interesting to stress that in Tan et al.'s work [19], no segment was revealed as having a significantly dominant impact on the accuracy of the GRF estimation. This may be due to the fact that the authors implemented a machine learning framework for the estimation of GRF from simulated raw data of segment-mounted MIMUs, without attributing a priori different weights to specific sensors. This machine learning framework may also explain the fact that the magnitude of positioning errors (0.1 m vs 0.02 m in the present study) had a negligible influence on the accuracy of the GRF estimation.

The results of the sensitivity analysis performed on bCoM accelerations in the present study advocate the need for an accurate detection of MIMU positions, especially for the trunk, the sound thigh, and the sound shank along both the V and the AP directions. The important influence of the correct localization of the trunk and sound thigh-mounted MIMUs might be explained by the fact that they are the heaviest segments of the body and that the bCoM acceleration is estimated using a weighted average of sCoM acceleration based on their mass. The sound shank influence may result from the higher angular velocity of shank segments (almost twice as that of the other included segments) while walking

and the relatively high mass of the sound shank compared to its prosthetic counterpart. Limiting the errors in the estimation of sCoM accelerations, especially at the shank, is expected to have a positive impact on the accuracy of the bCoM acceleration estimates. Indeed, if particular attention is given to the identification of the positions of these three MIMUs in the AP and V directions, the variations in  $rRMSE$  previously observed may be reduced from 2.8%, 2.3%, and 1.4% to 0.9%, 0.7%, 0.6% in AP, ML, and V directions, respectively.

### 4.3 Limitations and perspectives

The generalizability of the discussed results must be interpreted at the light of the following considerations: first, a larger cohort of participants is needed to confirm present findings. Second, simulated errors in the identification of MIMU positions were introduced along the axes of the reference frame  $R_{OMC}$ . Future studies might replicate the described approach by simulating erroneous MIMU position identification along the axes of the considered body segment anatomical frames. It is worth to underline, however, that the errors introduced covered a cubic zone centered on the correct location of the MIMU's origin during the static posture. Furthermore, the static calibration phase was performed with the patient standing in an upright posture facing the direction of progression, so that segment anatomical axes can be assumed to be aligned with those of the global frame  $R_{OMC}$  at the beginning of the walking trial (one axis aligned with the gravity and one axis with the direction of progression). It can be thus assumed that in case the anatomical frame should be considered instead of  $R_{OMC}$ , the position identification errors would cover a similar cubic volume, leading to negligible variations in the obtained sensitivities. Moreover, the 0.02-m range of errors used to simulate erroneous MIMU position identifications is a conservative value, being the maximum error observed (see [Supplementary information](#)), and thus representing a worst-case scenario presumably overcoming the range of errors that would be observed in practice.

It is interesting to note that the variations in  $rRMSE$  may also be negative (Table 6), indicating that the erroneous identification of MIMU positions may lead to an improvement of the estimated acceleration of the bCoM when compared to force platforms. This may be induced either by compensations of inaccuracies due to the bCoM approximation from five

sCoMs with localization errors, or by inaccuracies of the inertial model, resulting in poor positions of the sCoM in their respective segment anatomical frames. In this respect, it is worth noting that there is a lack of validated inertial models for people with lower-limb amputation in the literature and further studies should focus on this aspect.

Finally, in the present study, the impact of MIMU orientation errors was not investigated despite the latter was found to critically impact the accuracy of GRF estimation in [19]. It should be considered, however, that in Tan et al.'s work [19], simulated raw MIMU signals were used as inputs of a machine learning model and were not expressed in a global or anatomical reference frame. Therefore, modifying the sensor-to-segment orientations had a definitive impact on the output of the sensors in their local frames, and in turn, on the inputs of the machine learning algorithm. Conversely, in the MIMU-based framework proposed in the present study, the MIMU data are first expressed in a global reference frame prior to being used for the estimation of sCoM and bCoM accelerations. Modifying the sensor-to-segment orientation should therefore not impact the accuracy of the estimated bCoM accelerations. However, errors typical of sensor-fusion filters used to obtain MIMU 3D orientation remain to be considered. It should be noted that these errors are generally in the order of magnitude of the degrees and are therefore expected to have a minor impact with respect to what is reported in Tan et al.'s work [19]. Further studies should verify this hypothesis and quantify the impact of orientation errors on both sCoM and bCoM accelerations.

## 5 Conclusion

The present paper investigated the impact of an erroneous identification of the positions of a set of body-mounted MIMUs on the estimation accuracy of sCoM and bCoM accelerations during walking in a person with transfemoral amputation. An optical motion capture system and force plates were used as reference for sCoM and bCoM accelerations estimates, respectively. The performed sensitivity analyses allowed to identify the MIMU locations and axes which were the most critical for an accurate estimation of both sCoM and bCoM accelerations. Specifically, an accurate identification of MIMUs positioned on the trunk and sound lower limbs along the anteroposterior and vertical axes was proved to reduce the variability of the accuracy of the estimated bCoM acceleration to values lower than 1%. These preliminary results indicate that although the influence of MIMU position identification errors depends on the considered movement/segment, when gait is considered, special attention should be paid when identifying the position of wearable sensors on the different body segments, especially for the AP and V directions and for shank-mounted MIMUs. In conclusion, the present study

provides an interesting piece of information for those who are interested in the use of wearable inertial sensors for monitoring human locomotion, with particular reference to the estimation of sCoM- and bCoM-related quantities and open a new perspective in the use of wearable technologies for ecological assessment of patients' locomotion.

**Funding** Research reported in this publication was partially supported by grants from the Fédération des Amputés de Guerre de France and the Université Franco-Italienne (Call VINCI 2018 – C2-881, attributed to E. Simonetti). Study sponsors did not have a role in the study design, collection, analysis, and interpretation of data; writing of the manuscript; or the decision to submit the manuscript for publication.

## Declarations

**Ethical approval** All procedures performed in studies involving human participants were in accordance with the ethical standards of the national research committee (CPP NX06036) and with the 1964 Helsinki declaration and its later amendments or comparable ethical standards.

**Consent to participate** Informed consent was obtained from the participant included in the study.

**Consent to publish** The participant provided informed consent for the publication of his photographs in Fig. 1 as well as on the [Supplementary information](#).

**Conflict of interest** The authors declare no competing interests.

## References

1. Cavagna GA, Kaneko M (1977) Mechanical work and efficiency in level walking and running. *J Physiol* 268:467–481. <https://doi.org/10.1113/jphysiol.1977.sp011866>
2. Minetti AE (1998) The biomechanics of skipping gaits: a third locomotion paradigm? *Proc R Soc B Biol Sci* 265:1227–1235. <https://doi.org/10.1098/rspb.1998.0424>
3. Minetti AE, Cisotti C, Mian OS (2011) The mathematical description of the body centre of mass 3D path in human and animal locomotion. *J Biomech* 44:1471–1477. <https://doi.org/10.1016/j.jbiomech.2011.03.014>
4. Askew GN, McFarlane LA, Minetti AE, Buckley JG (2019) Energy cost of ambulation in trans-tibial amputees using a dynamic-response foot with hydraulic versus rigid 'ankle': insights from body centre of mass dynamics. *J Neuroeng Rehabil* 16:39. <https://doi.org/10.1186/s12984-019-0508-x>
5. Iida H, Yamamuro T (1987) Kinetic analysis of the center of gravity of the human body in normal and pathological gaits. *J Biomech* 20:987–995. [https://doi.org/10.1016/0021-9290\(87\)90328-9](https://doi.org/10.1016/0021-9290(87)90328-9)
6. Tesio L, Rota V (2019) The motion of body center of mass during walking: a review Oriented to Clinical Applications. *Front Neurol* 10:999. <https://doi.org/10.3389/fneur.2019.00999>

7. Agrawal V, Gailey R, O'Toole C, Gaunaud I, Dowell T (2009) Symmetry in external work (SEW): a novel method of quantifying gait differences between prosthetic feet. *Prosthetics Orthot Int* 33: 148–156. <https://doi.org/10.1080/03093640902777254>
8. Tesio L, Rota V (2019) The motion of body center of mass during walking: a review Oriented to Clinical Applications. *Front Neurol* 10:1–22. <https://doi.org/10.3389/fneur.2019.00999>
9. Pavei G, Seminati E, Cazzola D, Minetti AE (2017) On the estimation accuracy of the 3D body center of mass trajectory during human locomotion: inverse vs. forward dynamics. *Front Physiol* 8:1–13. <https://doi.org/10.3389/fphys.2017.00129>
10. Catena RD, Chen SH, Chou LS (2017) Does the anthropometric model influence whole-body center of mass calculations in gait? *J Biomech* 59:23–28. <https://doi.org/10.1016/j.jbiomech.2017.05.007>
11. Pillet H, Bonnet X, Lavaste F, Skalli W (2010) Evaluation of force plate-less estimation of the trajectory of the centre of pressure during gait. Comparison of two anthropometric models. *Gait Posture* 31:147–152. <https://doi.org/10.1016/j.gaitpost.2009.09.014>
12. Bergamini E, Ligorio G, Summa A, Vannozzi G, Cappozzo A, Sabatini A (2014) Estimating orientation using magnetic and inertial sensors and different sensor fusion approaches: accuracy assessment in manual and locomotion tasks. *Sensors* 14:18625–18649
13. Sabatini AM (2011) Estimating three-dimensional orientation of human body parts by inertial/magnetic sensing. *Sensors* 11: 1489–1525. <https://doi.org/10.3390/s110201489>
14. Madgwick SOH, Harrison AJL, Vaidyanathan A (2011) Estimation of IMU and MARG orientation using a gradient descent algorithm. In: *IEEE Int. Conf. Rehabil. Robot*, pp 1–7. <https://doi.org/10.1109/ICORR.2011.5975346>
15. Ligorio G, Bergamini E, Truppa L, Guaitolini M, Raggi M, Mannini A, Sabatini AM, Vannozzi G, Garofalo P (2020) A wearable magnetometer-free motion capture system: innovative solutions for real-world applications. *IEEE Sensors J* 20:8844–8857. <https://doi.org/10.1109/JSEN.2020.2983695>
16. Shahabpoor E, Pavic A, Brownjohn JMW, Billings SA, Guo LZ, Bocian M (2018) Real-life measurement of tri-axial walking ground reaction forces using optimal network of wearable inertial measurement units. *IEEE Trans Neural Syst Rehabil Eng* 26:1243–1253. <https://doi.org/10.1109/TNSRE.2018.2830976>
17. Lintmeijer LL, Faber GS, Kruk HR, van Soest AJK, Hofmijster MJ (2018) An accurate estimation of the horizontal acceleration of a rower's centre of mass using inertial sensors: a validation. *Eur J Sport Sci* 18:940–946. <https://doi.org/10.1080/17461391.2018.1465126>
18. Simonetti E, Bergamini E, Vannozzi G, Bascou J, Pillet H (2021) Estimation of 3D body center of mass acceleration and instantaneous velocity from a wearable inertial sensor network in transfemoral amputee gait: a case study. *Sensors* 21:3129. <https://doi.org/10.3390/s21093129>
19. Tan T, Chiasson DP, Hu H, Shull PB (2019) Influence of IMU position and orientation placement errors on ground reaction force estimation. *J Biomech* 97:109416. <https://doi.org/10.1016/j.jbiomech.2019.109416>
20. Basel J, Simonetti E, Bergamini E, Bascou J, Vannozzi G, Pillet H (2020) Definition of an optimal model based on segments' contribution for the estimation of the acceleration of the center of mass in people with lower-limb amputation. *Comput Methods Biomech Biomed Engin* 23:S25–S27. <https://doi.org/10.1080/10255842.2020.1811499>
21. Al Abiad N, Pillet H, Watier B (2020) A mechanical descriptor of instability in human locomotion: experimental findings in control subjects and people with transfemoral amputation. *Appl Sci* 10:840. <https://doi.org/10.3390/app10030840>
22. Basel J, Simonetti E, Bergamini E, Pillet H (2020) On the impact of the identification of inertial sensors location on the estimation of segment and body centers of mass in transfemoral amputees: a sensitivity study, *IEEE DataPort*. <https://doi.org/10.5281/zenodo.4058434>
23. Winter DA (1979) *Biomechanics of human movement*. Wiley, New York
24. Ren L, Jones RK, Howard D (2008) Whole body inverse dynamics over a complete gait cycle based only on measured kinematics. *J Biomech* 41:2750–2759. <https://doi.org/10.1016/j.jbiomech.2008.06.001>
25. J. Goupy, L. Creighton, *Introduction aux plans d'expériences - 3ème édition*, Paris, 2006.

**Joseph Basel** graduated from Université de Paris and Arts et Métiers (Paris, France) in 2020 with a master in Biomedical Engineering. He has a background in biomechanics and holds keen interests in the area of human motion analysis and rehabilitation.

**Emeline Simonetti** received a joint PhD in Biomechanics at Arts et Métiers (Paris, France) and Foro Italico (Rome, Italy). Her research aims at developing wearable methods for the assessment of people with lower-limb amputation.

**Elena Bergamini** received a joint PhD in Bioengineering at the University of Bologna (Italy) and Arts et Métiers ParisTech (France) in 2011. Her research concerns the development of methods to assess persons' motor function.

**Hélène Pillet** has a PhD in Biomechanics (2006) and an accreditation to supervise research (2015). Her research involves motion analysis for the understanding of musculoskeletal systems for clinical evaluation and rehabilitation.